PAPER

Thiolated polyglycerol sulfate as potential mucolytic for muco-obstructive lung diseases†‡

Justin Arenhoevel,§[a] Aditi Kuppe, [iD] §[b,c] Annalisa Addante, [iD] [b,c] Ling-Fang Wei,[a,f] Nico Boback,[a,f] Cosmin Butnarasu,[a,f] Yinan Zhong, [iD] [a] Christine Wong,[b,c] Simon Y. Graeber, [iD] [b,c,d] Julia Duerr, [iD] [b,c] Michael Gradzielski, [iD] [e] Daniel Lauster, [iD] *[a,f] Marcus A. Mall [iD] *[b,c,d] and Rainer Haag [iD] *[a]

Increased disulfide crosslinking of secreted mucins causes elevated viscoelasticity of mucus and is a key determinant of mucus dysfunction in patients with cystic fibrosis (CF) and other muco-obstructive lung diseases. In this study, we describe the synthesis of a novel thiol-containing, sulfated dendritic polyglycerol (dPGS-SH), designed to chemically reduce these abnormal crosslinks, which we demonstrate with mucolytic activity assays in sputum from patients with CF. This mucolytic polymer, which is based on a reportedly anti-inflammatory polysulfate scaffold, additionally carries multiple thiol groups for mucolytic activity and can be produced on a gram-scale. After a physicochemical compound characterization, we compare the mucolytic activity of dPGS-SH to the clinically approved *N*-acetylcysteine (NAC) using western blot studies and investigate the effect of dPGS-SH on the viscoelastic properties of sputum samples from CF patients by oscillatory rheology. We show that dPGS-SH is more effective than NAC in reducing multimer intensity of the secreted mucins MUC5B and MUC5AC and demonstrate significant mucolytic activity by rheology. In addition, we provide data for dPGS-SH demonstrating a high compound stability, low cytotoxicity, and superior reaction kinetics over NAC at different pH levels. Our data support further development of the novel reducing polymer system dPGS-SH as a potential mucolytic to improve mucus function and clearance in patients with CF as well as other muco-obstructive lung diseases.

Introduction

Airway mucus plugging is a key feature of muco-obstructive lung diseases such as cystic fibrosis (CF), chronic obstructive pulmonary disease (COPD) and asthma, and plays a key role in the onset and progression of chronic inflammation and infection leading to structural lung damage.[1–3] The highly glycosylated large secreted mucins MUC5B and MUC5AC with a fiber length of 0.2 to 10 μm are the main components of airway mucus.[1,4] These fibers form intermolecular crosslinks *via* disulfide bonds of cysteines, and thereby develop a stable mucus hydrogel that covers and protects airway surfaces.[5,6] In muco-obstructive lung diseases such as CF, these crosslinks are substantially increased due to oxidation of free thiol groups of mucins by reactive oxygen species (ROS), which are generated by neutrophils during the process of airway inflammation.[6–8] The viscoelasticity of the mucus hydrogel is thereby increased leading to mucus stiffening, impaired mucociliary clearance and mucus plugging of the airways.[2,9] Consequently, this makes excess mucin disulfide crosslinks a therapeutic target of high interest in muco-obstructive lung diseases.[10] Currently, *N*-acetylcysteine (NAC) is the only thiol-containing mucolytic approved for the treatment of CF. However, NAC failed to show mucolytic effects *in vivo*.[6,11]

Current research on new mucolytics is focused on small molecule reducing agents with increased mucolytic activity compared to NAC. A thiol-saccharide (MUC-031) showed faster and stronger mucolytic activity than NAC in CF sputum and

[a]Freie Universität Berlin, Institute of Chemistry and Biochemistry, SupraFAB, Altensteinstr. 23a, 14195 Berlin, Germany. E-mail: daniel.lauster@fu-berlin.de, haag@chemie.fu-berlin.de

[b]Charité – Universitätsmedizin Berlin, Department of Pediatric Respiratory Medicine, Immunology and Critical Care Medicine, Augustenburger Platz 1, 13353 Berlin, Germany. E-mail: marcus.mall@charite.de

[c]German Center for Lung Research (DZL), Associated Partner Site, 13353 Berlin, Germany

[d]Berlin Institute of Health at Charité – Universitätsmedizin Berlin, Charitéplatz 1, 10117 Berlin, Germany

[e]Technische Universität Berlin, Institute of Chemistry, Straße des 17. Juni 124, 10623 Berlin, Germany

[f]Freie Universität Berlin, Institute of Pharmacy, Biopharmaceuticals, Kelchstraße 31, 12169 Berlin, Germany

†Dedicated to Professor George M. Whitesides on the occasion of his 85th birthday.

‡Electronic supplementary information (ESI) available. See DOI: https://doi.org/10.1039/d4bm00381k

§Both authors contributed equally.

reduced airway mucus plugging and inflammation in a mouse model for muco-obstructive lung disease.[6,12] Similar findings were reported for the mucolytic compound P3001,[13] and tris(2-carboxyethyl)phosphine (TCEP), which demonstrated effective reduction of mucus plugging in a mouse model of asthma by reducing disulfides in MUC5B and MUC5AC.[14] In addition to the design of new mucolytics, various attempts have also been made to develop new lung delivery formulations using biocompatible scaffolds that increase the transport of mucolytics or natural fiber-based polymers, which themselves disentangle abnormal mucin networks.[15–18]

In contrast to this increasing search for small molecule mucolytics or better delivery technologies, we herein propose the use of dendritic polyglycerol scaffolds covalently connected to multiple mucolytically acting thiols. Dendritic polyglycerol (dPG) or its sulfated analogue (dPGS) are spherical nanoparticles (Scheme 1B) with a high density of functional groups, that are radially exposed to its surface.[19] Besides demonstrating a high water solubility, highly sulfated dPGS also demonstrates biological activities, such as antiviral properties against SARS-CoV-2[20] and other viruses,[21–23] as well as effective anti-inflammatory properties by leucocyte hitchhiking and interfering with immune cascades.[24–26] These antiviral and anti-inflammatory properties might also be beneficial for patients with CF and other muco-obstructive lung diseases.

The aim of this study was to assess the novel concept of multifunctional polymer mucolytics and synthesize a reducing agent with potent mucolytic activity based on a polyelectrolyte scaffold by thiolation of a highly sulfated polymer backbone. We tested physicochemical properties, effects on viability of

primary epithelial cells and the mucolytic efficacy of our novel compound dPGS-SH using rheological measurements and western blot analysis of sputum samples from patients with CF.

Materials and methods

Materials

All Chemicals were purchased from Sigma Merck KGaA (Darmstadt, Germany) and/or its affiliates and used without any further purification, unless otherwise stated. *N,N*-Dimethylformamide (DMF), dithiothreitol (DTT) and mouse monoclonal antibody against human MUC5AC (MA5-12178) were purchased from Thermo Fisher Scientific Inc. (Waltham, MA, USA). Mouse monoclonal antibody against human MUC5B (sc-393952) and secondary antibody goat Anti-Mouse Immunoglobulins/HRP were purchased from Santa Cruz Biotechnology (Dallas, TX, USA) and Agilent Dako (Glostrup, Denmark) respectively. PneumaCult ALI medium was purchased from STEMCELL Technologies (Cologne, Germany). Zombie aqua antibody was purchased from BioLegend (San Diego, CA, USA). 2-Iminothiolane hydrochloride was purchased from ABCR GmbH (Karlsruhe, Germany) and *N*-acetylcysteine (NAC) was purchased from BioGems International Inc. (Westlake Village, CA, USA). Dendritic polyglycerol (dPG-OH) was obtained from glycidol polymerization as reported in literature.[27] Amine functionalized dendritic polyglycerol (dPG-NH$_2$, DF = 10%, 10.5 kDa) was synthesized as previously described in our group.[28] Cyanine5-labeled dPGS-NH$_2$ (dPGS-Cy5) was synthesized as described before[29]
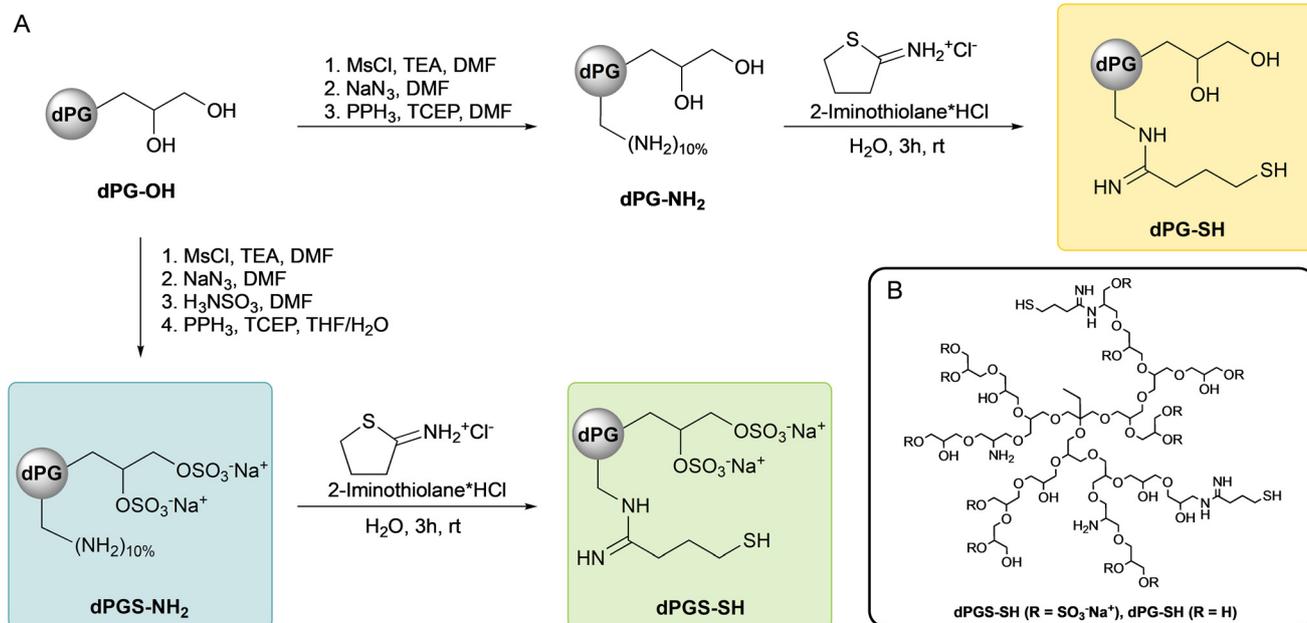
Scheme 1 Synthetic route of dPGS-SH and dPG-SH. (A) dPGS-NH$_2$ (blue box) was synthesized in 60 g scale by mesylation, azidation, sulfation and Staudinger reduction of dPG. dPG-NH$_2$ was synthesized similarly in small scale excluding the sulfation step. Thiolation was finally performed using 2-iminothiolane in aqueous solutions to obtain dPGS-SH (green box) and dPG-SH (yellow box). (B) Idealized schematic representation of dPGS-SH and dPG-SH.

and obtained with a dye-to-polymer ratio of 0.41 as determined by UV-VIS spectroscopy.

Instruments

The JEOL Eclipse 500 MHz (Tokyo, Japan) instrument was used to measure the ^{1}H NMR spectra of all the compounds reported here, recorded at 300 K. Chemical shifts δ were reported in ppm and the deuterated solvent peak (D_2O) was used as a standard. Elemental analyses of all relevant compounds in this work were performed with Vario EL CHNS element analyzer (Elementar Analysensysteme GmbH (Langenselbold, Germany)). Dynamic light scattering (DLS) and zeta potential were measured on a Malvern zetasizer nano ZS ZEN 3600 ((Malvern Instruments Ltd, Worcestershire, UK)) using a He–Ne laser ($\lambda = 532$ nm) at 178° backscatter and automated attenuation at 25 °C. DLS samples were prepared in PBS (10 mM, pH = 7.4) with a concentration of 1 mg mL^{-1} and samples for zeta potential were prepared in 10 mM PB (pH = 7.4) at concentrations of 5 mg mL^{-1}. Images in the diffusion studies by FRAP were acquired with a Leica TCS SP8 confocal microscope (Leica Microsystems) with a 63× oil immersion objective, NA 1.4. Sequential acquisition was performed at 256 × 256 pixels per image and a scanning speed of 1800 Hz, with a zoom factor of 7.5 and a pixel size set to 96 × 96 nm. All acquisition settings were set equally for each sample. Bleaching for FRAP experiments was done with the HeNe 633 nm line set to 100% power. UV/Vis measurements were performed on an AGILENT Cary 8454 UV-visible spectrophotometer, using half-micro disposable polystyrene cuvettes. Rheology was measured on a Kinexus Pro+ Rheometer (Netzsch GmbH, Selb, Germany) using a stainless-steel cone-plate geometry (cone diameter 20 mm, cone-angle 1°). Western blots were performed using a vacuum blotter (MP Biomedicals, Irvine, CA, USA) and imaged using a ChemiDoc™ MP Imaging System (Bio-Rad Laboratories Inc., Hercules, CA, USA).

Synthesis of dPGS-NH$_2$

dPG-OH (M_w = 10.5 kDa, 33.40 g, 3.2 mmol, 1.0 eq.) was dissolved in dry DMF (300 mL) and mixed with triethylamine (TEA) (9.42 mL, 12.98 g, 128 mmol, 40.0 eq.). Methanesulfonyl chloride (8.7 mL, 5.90 g, 51.5 mmol, 16.1 eq.) was added dropwise within 30 min at 0 °C. The solution was allowed to reach room temperature and stirred for 24 h. Azidation was performed *in situ* by the subsequent addition of NaN$_3$ (8.32 g, 128 mmol, 40 eq.) and the mixture was stirred at 70 °C for 72 h. Sulfamic acid (83.0 g, 0.855 mol, 270.0 eq.) was added subsequently and the mixture was stirred for additional 72 h at 60 °C. The mixture was filtered, and purification was performed by tangential flow filtration (TFF) in water (15 L) with a MWCO of 5 kDa, yielding dPGS-N$_3$ with a degree of sulfation (DS) of 83% (elemental analysis: N = 3.03, C = 22.98, S = 14.18, H = 4.58). Finally, reduction of azide groups was achieved by dissolving dPGS-N$_3$ (3.2 mmol, 1.0 eq.) in a H$_2$O/THF-mixture (30 : 70, v/v) to a volume of 1.0 L. Triphenylphosphine (33.6 g, 128 mmol, 40 eq.) was added slowly and the mixture was

stirred for 48 h at room temperature. TCEP (12.8 g, 44.8 mmol, 14.0 eq.) was added subsequently and the mixture was stirred for 24 h to assure a complete reduction. Precipitates were removed by filtration and the solution was neutralized with NaOH solution (2 M) and the crude product was purified by TFF in water (15 L) with a MWCO of 5 kDa. dPGS-NH$_2$ was obtained as yellow solid in a yield of 93%. ^{1}H NMR: (500 MHz, D$_2$O, δ (ppm)): 4.71–3.16 (m, polymer backbone), 1.34 (s, 2H, polymer starter), 0.81 (s, 3H, polymer starter).

Synthesis of dPGS-SH & dPG-SH

Thiolation of polymers dPGS-NH$_2$ and dPG-NH$_2$ was performed in similar conditions. Polymers were dissolved in H$_2$O (5 mM) and the pH was carefully adjusted to pH = 8.0 using 1 M NaOH. Solutions were purged with argon for 15 min and 2-iminothiolane HCl (0.5 eq. per NH$_2$-group) was added followed by equimolar amount of NaOH from a 1 M solution. The mixtures were purged for another 10 min, sealed carefully and then stirred for 3 h at room temperature. Solutions were neutralized using 1 M HCl and lyophilized. Products were obtained as viscous solid (dPG-SH) or colorless solid (dPGS-SH) in quantitative amounts. ^{1}H NMR (dPG-SH, 500 MHz, D$_2$O, δ (ppm)): 4.10–3.30 (m, polyglycerol backbone), 3.28 (s, 2H, –CH$_2$SH), 2.67 (s, 2H, –CH$_2$CH$_2$SH), 2.14 (s, 2H, –CH$_2$CH$_2$CH$_2$SH), 1.35 (s, 2H, polymer starter), 0.87 (s, 3H, polymer starter). ^{1}H NMR (dPGS-SH, 500 MHz, D$_2$O, δ (ppm)): 4.72–3.30 (m, polymer backbone), 3.24 (s, 2H, –CH$_2$SH), 2.42 (s, 2H, CH$_2$CH$_2$SH), 1.40 (s, 2H, polymer starter), 0.89 (s, 3H, polymer starter).

Diffusivity measurements *via* fluorescence recovery after photobleaching (FRAP)

A dPGS-Cy5 stock solution was prepared in 10 mM PBS, pH = 7.4 at a final concentration of 100 µM (*i.e.*, expressed as Cy5 concentration). Samples for FRAP diffusivity measurements were prepared by diluting the dPGS-Cy5 stock solution in healthy or CF mucus to a final concentration of 2.5 µM. Samples were homogenized by vortexing for 1 min. Imaging samples were prepared by pipetting 30 µL samples onto chambered glass coverslips (Ibidi, µ-Slide, 170 µm ± 5 µm). A circular region of interest (ROI, 40.8 µm^2) was selected within the analyzed field. A time-series analysis was programmed with the following settings: prebleaching images recorded at 2% laser transmission, immediately followed by bleaching. The recovery step spanned a total duration of 67.8 s. During the initial postbleach step (7.8 s), 100 frames were acquired; this was followed by a s (10 s), and a third (50 s) step, each acquiring 10 frames in total. The diffusivity data from FRAP measurements were computed as previously described.[30] The fluorescence intensity inside the ROI was normalized to the prebleach intensity. Then, a least squares fit was applied to obtain the diffusion time, τ_D. The diffusion coefficient (D) was calculated using the eqn (S4).‡ Each FRAP measure was repeated 4 times.

Ellman's assay

Ellman's assay was performed with mercaptoethanol as a calibration standard. Briefly, 8 standard sample solutions were prepared in PB buffer (10 mM, pH = 8.0, containing 10 mM EDTA) in the range between 0.025 mM and 1.0 mM. DTNB was dissolved in the same buffer to a concentration of 4 mg mL^{-1}. Measuring samples were composited of 2.5 mL buffer, 250 μL sample solution with known concentration and 50 μL of the prepared DTNB solution.

After an incubation time of 15 min the absorption was measured at 412 nm and the obtained maxima were plotted against the concentration. Considering the linear equation, thiol quantification of unknown samples was thereby calculated in relation to the obtained standard. All samples were measured in triplicate at 25 °C in disposable polystyrene cuvettes.

Stability studies of dPGS-SH

Stability of thiol compounds was determined by monitoring the relative amount of thiol groups per molecule over time using the Ellman's assay. Dry samples were aliquoted and stored in sealed glass vials at −4 °C, 6 °C and 25 °C and only opened prior to the measurement. Samples were dissolved to a concentration of 0.1 mM and thiols were quantified according to a mercaptoethanol standard. Dissolved samples were stored in PBS buffer (pH = 7.4, 10 mM) at a concentration of 0.1 mM (V = 1000 μL). Solutions were purged with argon for 10 min and then sealed carefully. To assure an effective and long-term oxygen exclusion, samples were sealed and stored in argon saturated gas-tight bags at 6 °C or 25 °C. The effect of oxygen exclusion was not investigated for samples stored at 37 °C.

Kinetic constant determination of reducing agents

Different thiol-based reducing agents were investigated in kinetic experiments with the Ellman's reagent (DTNB). The calibration and determination of the extinction coefficient was performed with a dilution series of 12 concentrations between 0 and 40 μM using 2-mercaptoethanol. Sample solutions (100 μL) were prepared in calcium- and magnesium free DPBS (1 mM, pH = 7.4), mixed with DTNB solution (0.2 mM or 0.02 mM in DPBS (1 mM, pH = 7.4)) and absorbance at 412 nm was measured after 15 min. To determine the kinetic constant, sample solutions (100 μL) of dPGS-SH, DTT (0.005 mM, 0.01 mM, 0.015 mM, 0.02 mM) and NAC (0.05 mM, 0.1 mM, 0.15 mM, 0.2 mM) were mixed with the DTNB solution (100 μL) and the absorbance at 412 nm was measured directly in intervals of 10 s until saturation was reached. Using the resulting TNB^{2-} concentration over time and the linear absorbance increase of the reactions a reaction constant (k) was calculated with the second order rate law.

Cell viability assay

Primary human nasal epithelial cells were obtained by nasal brushings. All experiments were performed in accordance with the Declaration of Helsinki, the sampling of phNECs was approved by the ethics committee of the Charité – Universitätsmedizin Berlin (EA2/220/18) and written informed consent was obtained from all patients and healthy controls. Cultivation of cells was performed by the conditionally reprogrammed cell culture method as previously described.[31] In brief, brushed cells were expanded in co-culture with irradiated mouse 3T3 fibroblasts in the presence of RhoA kinase inhibitor Y-27632. Epithelial cells were seeded at passage 2 or 3 on human placental type IV collagen-coated, 0.4 μm pore size mini transwell 0.33 cm^2 supports (Sigma Merck, Darmstadt, Germany) at a density of 200 000 cells per cm^2 in PneumaCult ALI medium and differentiated at air liquid interphase (ALI) for 3–4 weeks, as previously described.[32] Cells were washed 24 h before the treatment to allow some mucus to accumulate. Cell cultures were treated with 0.75 μl of freshly prepared 5 mM solution dPGS-SH or 0.75 μl PBS. 48 h after treatment, cells were stained with Zombie aqua for 30 min at 4 °C and fixed *in situ*. Cells were dissociated from the transwell membrane using trypsin and analyzed *via* flow cytometry.

Sputum collection

Spontaneously expectorated sputum samples were collected from patients with CF according to protocols approved by the ethics committee of the Charité – Universitätsmedizin Berlin (EA2/016/18). Written informed consent to participate in this study was provided by all participants, parents or legal guardians. All experiments were performed in accordance with the Declaration of Helsinki. Demographics and clinical characteristics of study participants are shown in ESI Table S1.‡ CF patients spontaneously expectorated sputum into a sputum collection cup. Any easily visible saliva layers in the sputum samples were removed by gentle pipetting prior to further processing as previously described.[33] Sputum samples used for rheological analysis were stored at 4 °C for up to 24 h. Sputum samples used for western blot analysis were stored at −20 °C to be analyzed at a later date.

Sputum rheology

As recently shown, proteases present in sputum samples can have an effect on its viscoelastic properties.[12] We therefore treated all samples with a protease inhibitor (PI) prior to rheological treatment experiments. Undiluted sputum from patients with CF were then treated with freshly prepared 1 mM solution of dPGS-SH or PBS as control at 37 °C for 30 min and then quenched with iodoacetamide. The storage modulus (G') and loss modulus (G'') were determined by dynamic oscillatory macrorheological measurements with a Kinexus Pro+ Rheometer using a stainless-steel cone-plate geometry (cone diameter 20 mm, cone-angle 1°) as previously described.[33] Each measurement included an amplitude sweep (1 Hz, 0.01–100% strain) and a frequency sweep (2% strain, 10–0.1 Hz). G' and G'' were directly extracted from the linear viscoelastic region of the amplitude sweep. Fold changes of G' and G'' were determined by normalization of values obtained after treatment with mucolytic compounds by values obtained after

treatment with PBS alone to account to the variability of sputa obtained from different patients with CF.

Western blot

Mucin western blot was performed as previously described.[12,34] Briefly, sputum from CF patients was diluted at 1 : 5 in PBS and homogenized using a 1 mL syringe and 20 G cannula. Diluted sputum was treated with increasing concentration of NAC, dPGS-SH, dPG-SH and DTT (0.1–5 mM) at 37 °C for 30 min and then quenched with iodoacetamide. All solutions were prepared freshly and used immediately. Agarose gel electrophoresis using 0.8% agarose was combined with transfer onto a nitrocellulose membrane *via* vacuum. After loading the gels, proteins were separated on 0.8% agarose gel at 80 V (1.5 h) with Tris–acetate–EDTA/SDS buffer. For an efficient mucin transfer, the gel was reduced for 20 min in a solution containing 10 mM DTT and proteins were then transferred to nitrocellulose membranes by vacuum blotting. Blots were probed with a mouse monoclonal antibody against human MUC5B diluted at 1 : 1000 in 1% milk–PBS and mouse monoclonal antibody against human MUC5AC diluted at 1 : 1000 in 1% milk–PBS. The secondary antibody was a goat anti-mouse immunoglobulins/HRP, diluted 1 : 4000 in 1% milk–PBS. Detection was performed using ChemiDoc™ MP Imaging System. Multimer signal intensities were analyzed using Fiji[35,36] and normalized against PBS treated control.

Results and discussion

Synthesis, compound stability and reduction kinetics

By combining a high degree of sulfation (>80%) with a low degree of thiol groups, we developed a highly mucolytic polymer on an anti-inflammatory scaffold. Dendritic polyglycerol (dPG) was synthesized as described before,[27] obtaining a polymer scaffold with a molecular weight (M_w) of 10.0 kDa (M_w) and a polydispersity of 1.29. Using our well-established methods of mesylation, azidation, sulfation and subsequent Staudinger reduction,[28,37] we produced our precursor polymer dPGS-NH$_2$ in large scale (60 g synthesis). 2-Iminothiolane was previously shown to react with dPGS-NH$_2$ as well as other amine-functionalized polyglycerols in a fast, quantitative conversion forming a terminal thiol group.[38,39] By using lower equivalents of 2-iminothiolane (0.5 eq. per NH$_2$) in relation to amine functionalities on a polyglycerol moiety (10%) we assure a complete conversion, as confirmed by ^{1}H NMR (Fig. S1–S3‡), forming thiolated polyglycerol sulfate (dPGS-SH). The non-sulfated analogue polymer (dPG-SH) was synthesized similarly excluding the sulfation step (Scheme 1). Particle sizes of dPGS-SH (5.2 ± 0.1 nm) and dPG-SH (4.3 ± 0.1 nm) were determined by DLS (Fig. S4‡) and in similar size to the precursor polymer dPGS-NH$_2$ (4.1 ± 0.1 nm). As a consequence, we excluded the presence of polymer–polymer crosslinks that polymers with multiple thiol groups potentially could form. With particle diameters below 6 nm, we intend minimized steric interaction with human mucus, which has a significantly

wider mesh size even in pathologic sputum of patients with CF of approximately 70 nm[40] and assume steady diffusion through the mucus layer. To investigate the general diffusion capability of our polymer particles, diffusion of dye-labeled dPGS (dPGS-Cy5) in collected sputum samples was observed using a fluorescent recovery after photobleaching (FRAP) method (Fig. S5A‡). In CF sputum, polysulfate diffuses with 0.18 ± 0.09 μm^2 per second. As expected, diffusion is higher (approximately 15-fold) in healthy sputum samples (2.60 ± 0.47 μm^2) compared to CF mucus (Fig. S5B‡). Reduced diffusion in CF mucus can be attributed to several factors, including higher viscosity due to the approximately 11-fold higher protein content (39.1 *vs.* 3.6 mg mL^{-1}, quantified by BCA Protein assay), and a smaller mesh size. An increased polymer–mucus interaction in CF samples is also indicated by the reduced recovery of the fluorescent signal intensity.

The degree of sulfation (DS) was determined similar to previous reports[41,42] from sulfur elemental analysis of dPGS-NH$_2$. We obtained polymers with a DS of 83% resulting in a calculated molecular weight of 20.0 kDa for dPGS-SH. The zeta potentials of dPGS-SH and dPG-SH were determined to −44.1 ± 1 mV and −2.3 ± 0.5 mV, respectively, approving the high number of negatively charged sulfate groups in dPGS-SH. Due to the sulfation, we obtain a highly water-soluble compound with dPGS-SH, which makes it a suitable candidate for application as dry powder or liquid aerosol. Physicochemical properties of functionalized polymers were summarized in Table 1.

We quantified the number of free, reactive thiol groups of dPGS-SH and dPG-SH using the Ellman's assay. Herein, the model disulfide 5,5′-dithiobis-(2-nitrobenzoic acid) (DTNB) will be reduced by a thiol group quantitatively releasing the anion TNB^{2-} in a stoichiometric reaction (Scheme S1‡).[43] Monitoring this reduction by UV-Vis-spectroscopy enables the quantification of thiol groups per polymer in reference to a standard molecule. dPGS-SH and dPG-SH were determined to have 4.0 ± 0.1 and 3.3 ± 0.1 thiol groups per polymer, respectively. Moreover, the oxidation stability of dPGS-SH was observed over time by investigating polymer solutions stored under different conditions. Remarkably, at 37 °C the polymer oxidizes much slower than NAC (24 h) and DTT (8 h) keeping a free thiol content of more than 50% for more than 7 days (Fig. 1A). The slower oxidation of dPGS-SH might be explained by the charge repulsion of negatively charged polymers that consequently limits intermolecular disulfide bond formation. This observation is supported by DLS analysis of the particle size at the same storage conditions (Fig. S6‡). Herein we observe a slight increase followed by a stabilization of the particle size up to 120 h storage time. These data suggest that the oxidation process involves the formation of dimers or oligomers by intermolecular disulfide bonding. In addition, we assume that intramolecular disulfide bond formation of thiol groups in close proximity on the polymer surface contribute to the oxidation process. However, considering the decreased oxidation rate we expect a potentially higher *in vivo* stability of our polymeric mucolytics compared to NAC. Oxidation of the

Table 1 Physicochemical features of functionalized dendritic polyglycerols. Data represent the mean value of samples measured in triplicate ± standard deviation

	$M_w{}^a$ [kDa]	Particle size^b [nm]	PDI^b	Zeta potential [mV]	DS^c [%]	SH-groups^d
dPG-SH	10.5	4.3 ± 0.1	0.23 ± 0.02	−2.3 ± 0.5	—	3.3 ± 0.1
dPGS-NH$_{2(10\%)}$	20.0	4.1 ± 0.1	0.33 ± 0.09	−37.2 ± 1	83	—
dPGS-SH	20.0	5.2 ± 0.1	0.36 ± 0.23	−44.1 ± 1	83	4.0 ± 0.1

^{a} Calculated with eqn (S3)‡ based on the weight average molecular weight (M_w) of dPG-OH and the DF. ^{b} Determined as hydrodynamic diameter by DLS. ^{c} Determined by elemental analysis using eqn (S2).‡ ^{d} Determined by the Ellman's assay.
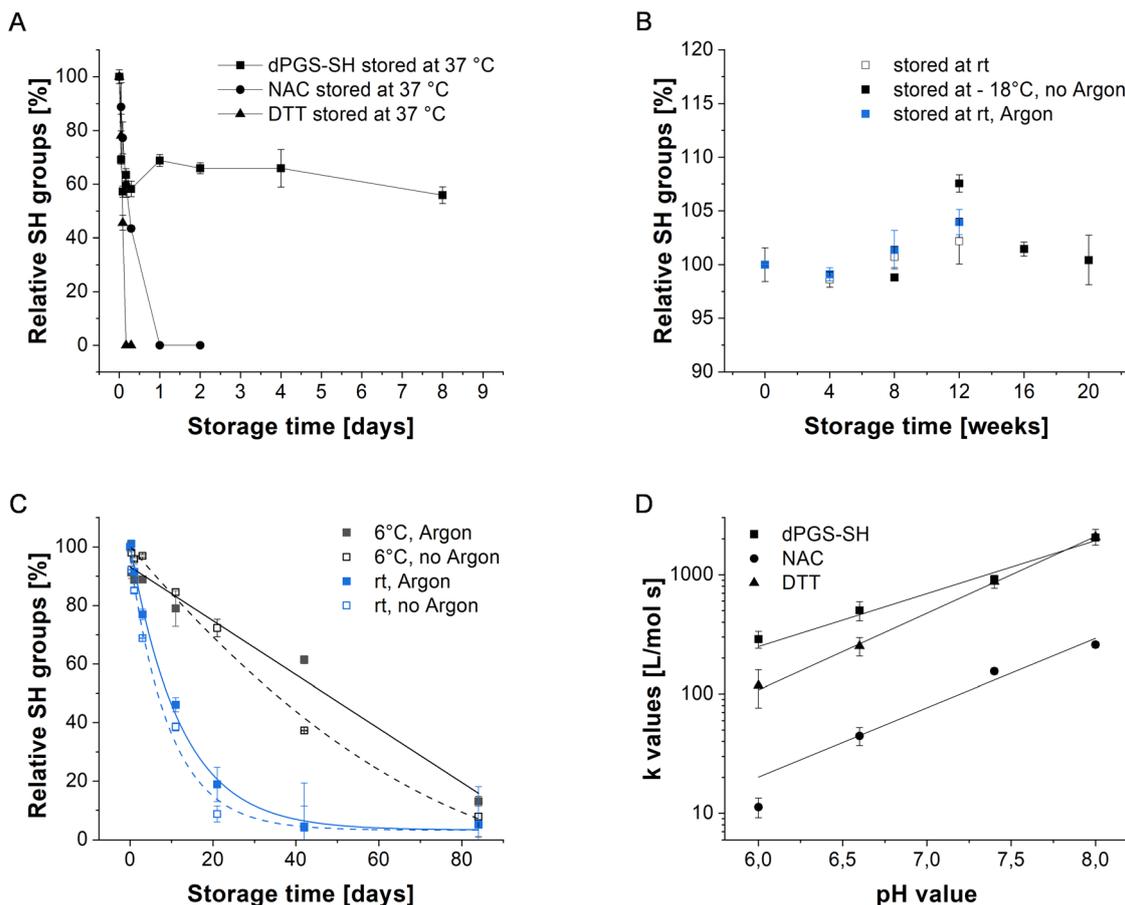
Fig. 1 Physicochemical properties and storage stability. (A) Oxidation stability of dPGS-SH, DTT or NAC at 37 °C dissolved in DPBS (10 mM, pH = 7.4). Data points represent the mean value of one sample measured in triplicate ± standard deviation. (B) Oxidation stability of dPGS-SH as lyophilized powder stored at 25 °C or −18 °C. Data points represent the mean value of one sample measured in triplicate ± standard deviation. (C) Oxidation stability of dPGS-SH dissolved in DPBS (10 mM, pH = 7.4) at 6 °C or 25 °C and in the presence or absence of argon to replace oxygen in the container. Data points represent the mean value of one sample measured in triplicate ± standard deviation. (D) Reaction kinetics of dPGS-SH, dithiothreitol (DTT) and N-acetylcysteine (NAC) in the reduction of the model disulfide DTNB at different pH values. K values were normalized to the respective number of SH-groups per molecule. Data points represent the mean value of three samples measured in triplicate ± standard deviation.

lyophilized powder could not be observed for dPGS-SH (Fig. 1B) even at room temperature, allowing long-term storage of our compound. The stability of dPGS-SH was additionally tested under experimental conditions in PBS (10 mM, pH = 7.4) of dissolved sample solutions at 25 °C and at 6 °C (Fig. 1C), resulting in low thiol oxidation within days. Oxygen exclusion by purging the solutions with argon led to even lower oxidation rates. However, subsequent experiments were

conducted with solid polymer samples that were used immediately after dissolving to their desired concentrations. Next, the reaction kinetics of dPGS-SH and dPG-SH with disulfides were monitored and compared to DTT and NAC using a DTNB-based kinetic assay at different pH values. The pH of airway surface liquid and exhaled breath condensate[44] was reported to be lower (pH ≤ 7) in patients with CF, indicating the need for reduction activity of mucolytics at different pH levels. As

shown in Fig. 1D, dPGS-SH clearly is advantageous over NAC in reducing the model disulfide DTNB. Below pH = 7 the reduction characteristics of dPGS-SH were even faster compared to DTT, which could be beneficial in the treatment of CF lung disease where the surface pH can reach levels below 7.

dPGS-SH does not cause cell toxicity in primary human nasal epithelial cells

Strong reduction potential can cause toxic *in vivo* effects[45,46] demonstrating the need for mucolytics that are both potent and biocompatible. To investigate cell toxicity of dPGS-SH *in vitro*, we treated highly differentiated primary human nasal epithelial cells (phNEC) grown in air–liquid interface (ALI) cultures with PBS and 5 mM solutions of dPGS-SH, which was the highest concentration used in the biological studies. By using a cell model with mucus-secreting cells, we investigate toxicity in a system mimicking the native environment of the surface that is in first contact with drugs applied as aerosol or dry powder to the lungs. We stained the cells with Zombie aqua to

analyze membrane integrity as a representative cell viability marker. Cells were analyzed *via* flow cytometry 48 h after treatment and no significant difference in cell viability between treatment with PBS and dPGS-SH was observed (Fig. 2). Lack of cell toxic effects of dPGS-SH up to 5 mM concentrations in highly differentiated human airway epithelial cell cultures grown under near-physiological conditions support the biocompatibility of our polymer.

dPGS-SH improves the viscoelastic properties of CF sputum

The viscoelastic properties in CF sputum are characterized by an increased storage modulus (G') caused by a more densely crosslinked mucus gel.[40,47] Thus, a therapeutic strategy is the decrease of G' from the elevated level towards the healthy state by cleaving the excessive number of disulfides. To investigate the reducing effect of dPGS-SH on viscoelastic properties of CF sputum samples, we performed rheological measurements and determined the storage modulus (G') and loss modulus (G''). Sputum samples from CF patients were treated with 1 mM solutions of dPGS-SH and compared to PBS treated control. In both treatment groups there was a high patient-to-patient variability (Fig. S8 and S9‡) and G' predominated over G'' indicating a gel-like behavior of all sputum samples that has been shown previously.[12,40,48] We found that 1 mM of dPGS-SH caused a significant decrease in G' ($P < 0.05$, Fig. 3A). For the viscous modulus G'' no change was observed in dPGS-SH treated sputum samples. In addition, mesh size was significantly increased in CF sputum samples treated with dPGS-SH (mean of 73.5 nm in PBS treated sputum samples to mean of 90.5 nm in dPGS-SH treated sputum samples ($P < 0.05$ Fig. 3C). Notably, the treatment with 5 mM dPGS-SH led to significant decrease in G' compared to the PBS treated control (Fig. S7‡). However, the observed effect was similar to 1 mM applications, suggesting that the maximum effect is achieved at 1 mM concentrations. As dPGS-SH has multiple thiol groups and could potentially act as a mucin crosslinker, treatment with dPGS-SH may also have the opposite effect and an increase the viscoelastic parameters of sputum samples.
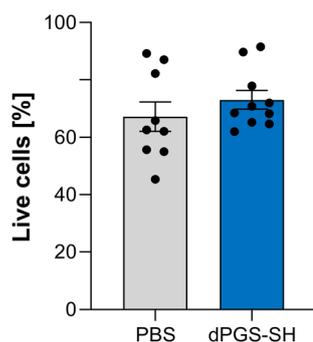

Fig. 2 Cell viability assay using live/dead stain (Zombie aqua) followed by analysis with flow cytometry. Cell viability of highly differentiated primary human nasal epithelial cells (phNEC) grown in air–liquid interface (ALI) shows no significant difference between treatment with 5 mM dPGS-SH solution compared to control treatment with PBS. Data represents the mean value of 8 to 10 samples with the standard error of the mean.
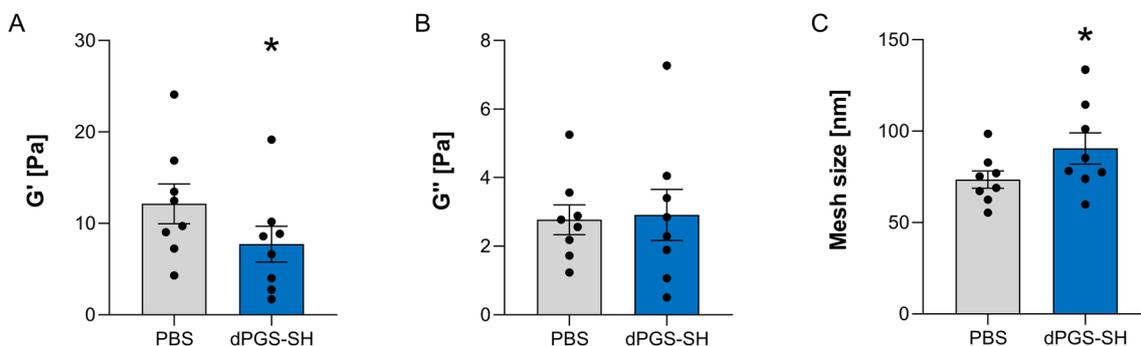
Fig. 3 Effect of dPGS-SH on the storage and loss modulus of sputum from patients with CF. Comparison of mucolytic effect of 1 mM solutions of dPGS-SH to PBS-treated control on storage modulus G' (A), loss modulus G'' (B) and mesh size (C). G' and G'' moduli of CF sputum samples are measured at the linear region of an amplitude sweep from 0.01–100% strain at 1 Hz. Mesh size was calculated from the storage modulus. Data represents the mean value of 6 to 9 samples ± the standard error of the mean. *$P < 0.05$, compared with PBS treated controls, performed with Wilcoxon test.
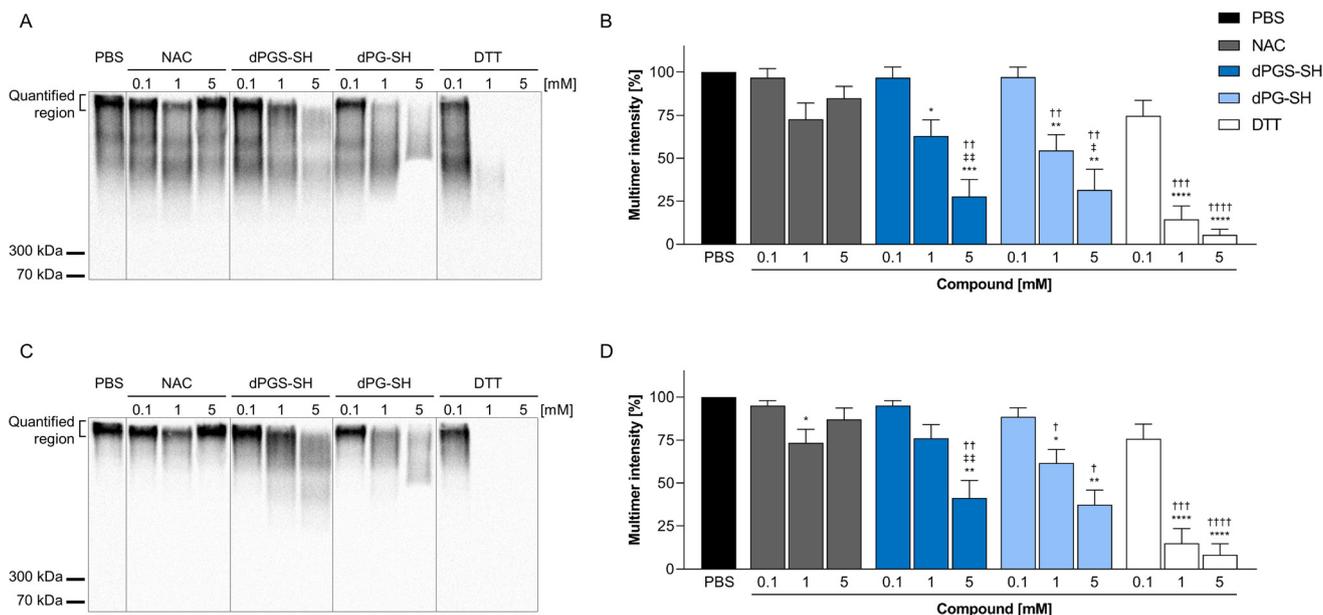
Fig. 4 Effect of *N*-acetylcysteine (NAC), dPGS-SH, dPG-SH and dithiothreitol (DTT) on the high molecular weight intensity of airway mucins. Representative western blot images of MUC5AC (A) and MUC5B (C). Quantification of multimer intensity of MUC5AC (B) and MUC5B (D) western blots, normalized to PBS treated controls. Data represents the mean value of 10 samples ± the standard error of the mean. $*P < 0.05$, $**P < 0.01$, $***P < 0.001$ and $****P < 0.0001$ compared with PBS treated controls; $†P < 0.05$, $††P < 0.01$, $†††P < 0.001$ and $††††P < 0.0001$ compared with 0.1 mM concentration of corresponding compound; $‡P < 0.05$ and $‡‡P < 0.01$ compared with 1 mM concentration, performed with Tukey's multiple comparisons test. Source data are provided in the ESI.‡

However, no gelation of the bare polymer solutions at the probed concentrations were observed and viewed in combination with the sputum rheology data, our results demonstrate a predominantly reducing effect of dPGS-SH.

dPGS-SH cleaves multimers of MUC5B and MUC5AC more effectively than NAC

In addition to rheological measurements, we performed western blot analyses of CF sputum samples treated with increasing concentrations (0.1 mM, 1 mM or 5 mM) of NAC, dPGS-SH, dPG-SH or DTT, and determined effects on high-molecular weight multimer intensity of MUC5B and MUC5AC compared to PBS treated controls. Our data show no change in high-molecular weight intensity for both mucins in samples treated with increasing concentrations of NAC, which is in agreement with previously published data,[12,13] and emphasizes the need for more effective mucolytic drugs. Both dPGS-SH and dPG-SH treated sputum samples showed a dose-dependent decrease of the high molecular weight intensity and a shift towards lower molecular weight mucins. Samples treated with 1 mM and 5 mM DTT showed almost a complete loss of signal (Fig. 4), which was also observed in previous studies.[12] The quantification of the high molecular weight region showed significant dose-dependent decrease in signal intensities for dPGS-SH, dPG-SH and DTT, but not for NAC treated samples (Fig. 4B and D). These results demonstrate a stronger mucolytic effect of dPGS-SH compared to NAC. The comparison of the mucolytic activity of dPG-SH and dPGS-SH

proves a thiol- and not sulfate-dependent mucin disassembly took place. This was further supported by the absence of mucin multimer degradation of samples treated with 5 mM dPGS-NH₂ (Fig. S10‡), emphasizing our polymers' inescapable reliance on thiol groups to achieve mucolytic effects.

Although similar mucolytic activities were also observed with small molecule reducing agents,[6,12–14] we here present a new class of polymeric reducing agent. As expected from previous reports, DTT also showed mucolytic effects in our experiments. However, DTT is associated with an enhanced endoplasmic reticulum stress and H₂O₂-induced toxicity[49,50] and thereby cannot be considered for *in vivo* application. Moreover, DTT might also lead to a loss of mucus transport abilities by its excessive reductive effect of mucin disulfides.

Conclusions

We introduce the concept of a novel macromolecular reducing agent based on dendritic polyglycerol sulfate (dPGS-SH) that is more active in cleaving mucin crosslinks than the clinically approved NAC. Moreover, dPGS-SH demonstrated higher stability compared to NAC even at 37 °C, and no toxicity on primary human nasal epithelial cells could be observed up to a tested concentration of 5 mM dPGS-SH. Notably, dPGS-SH caused a significant chemical reduction of mucin crosslinks in sputum of CF patients in a dose-dependent manner in western blot and improved viscoelastic properties in rheological experiments.

We herein present a new, multifunctional class of reducing agents based on a polymer which in comparison with previously reported mucolytics[12–14] clearly differentiates in terms of size, molecular weight and the presence of multiple, covalently bound thiol groups per molecule. Additional antiviral and anti-inflammatory features from the highly sulfated polymer can be expected from previous studies on dPGS.[20,21,24–26] Future investigations will address the effect of multifunctionality on mucolytic activity by comparing polymers with different sizes and degrees of thiolation. Our data supports future evaluation for potential clinical application as a novel mucolytic for the treatment of CF and other mucoobstructive lung diseases.

Data availability

The data supporting this article have been included as part of the ESI.‡

Conflicts of interest

There are no conflicts to declare.

Acknowledgements

Notes and references

1 R. C. Boucher, *N. Engl. J. Med.*, 2019, **380**, 1941–1953.

2 J. V. Fahy and B. F. Dickey, *N. Engl. J. Med.*, 2010, **363**, 2233–2247.

3 Z. Zhou-Suckow, J. Duerr, M. Hagner, R. Agrawal and M. A. Mall, *Cell Tissue Res.*, 2017, **367**, 537–550.

4 D. J. Thornton, K. Rousseau and M. A. McGuckin, *Annu. Rev. Physiol.*, 2008, **70**, 459–486.

5 D. J. Thornton, C. Sharpe and C. Ridley, *Ann. Am. Thorac. Soc.*, 2018, **15**, S154–S158.

6 S. Yuan, M. Hollinger, M. E. Lachowicz-Scroggins, S. C. Kerr, E. M. Dunican, B. M. Daniel, S. Ghosh, S. C. Erzurum, B. Willard, S. L. Hazen, X. Huang, S. D. Carrington, S. Oscarson and J. V. Fahy, *Sci. Transl. Med.*, 2015, **7**, 276ra227.

7 M. A. Mall, *Ann. Am. Thorac. Soc.*, 2016, **13**(Suppl. 2), S177–S185.

8 M. A. Mall, N. Mayer-Hamblett and S. M. Rowe, *Am. J. Respir. Crit. Care Med.*, 2020, **201**, 1193–1208.

9 D. B. Hill, B. Button, M. Rubinstein and R. C. Boucher, *Physiol. Rev.*, 2022, **102**, 1757–1836.

10 S. Y. Graeber and M. A. Mall, *Lancet*, 2023, **402**, 1185–1198.

11 G. Aldini, A. Altomare, G. Baron, G. Vistoli, M. Carini, L. Borsani and F. Sergio, *Free Radic. Res.*, 2018, **52**, 751–762.

12 A. Addante, W. Raymond, I. Gitlin, A. Charbit, X. Orain, A. W. Scheffler, A. Kuppe, J. Duerr, M. Daniltchenko, M. Drescher, S. Y. Graeber, A. M. Healy, S. Oscarson, J. V. Fahy and M. A. Mall, *Eur. Respir. J.*, 2023, **61**, 2202022.

13 C. Ehre, Z. L. Rushton, B. Wang, L. N. Hothem, C. B. Morrison, N. C. Fontana, M. R. Markovetz, M. F. Delion, T. Kato, D. Villalon, W. R. Thelin, C. R. Esther, Jr., D. B. Hill, B. R. Grubb, A. Livraghi-Butrico, S. H. Donaldson and R. C. Boucher, *Am. J. Respir. Crit. Care Med.*, 2019, **199**, 171–180.

14 L. E. Morgan, A. M. Jaramillo, S. K. Shenoy, D. Raclawska, N. A. Emezienna, V. L. Richardson, N. Hara, A. Q. Harder, J. C. NeeDell, C. E. Hennessy, H. M. El-Batal, C. M. Magin, D. E. Grove Villalon, G. Duncan, J. S. Hanes, J. S. Suk, D. J. Thornton, F. Holguin, W. J. Janssen, W. R. Thelin and C. M. Evans, *Nat. Commun.*, 2021, **12**, 249.

15 A. Bujan, S. del Valle Alonso and N. S. Chiaramoni, *Chem. Phys. Lipids*, 2020, **231**, 104936.

16 M. Guerini, P. Grisoli, C. Pane and P. Perugini, *Int. J. Mol. Sci.*, 2021, **22**, 891.

17 A. Malkawi, N. Alrabadi, R. Haddad, A. Malkawi, K. Khaled and A. C. Ovenseri, *Molecules*, 2022, **27**, 4611.

18 C. M. Fernandez-Petty, G. W. Hughes, H. L. Bowers, J. D. Watson, B. H. Rosen, S. M. Townsend, C. Santos, C. E. Ridley, K. K. Chu, S. E. Birket, Y. Li, H. M. Leung, M. Mazur, B. A. Garcia, T. I. A. Evans, E. F. Libby, H. Hathorne, J. Hanes, G. J. Tearney, J. P. Clancy, J. F. Engelhardt, W. E. Swords, D. J. Thornton, W. P. Wiesmann, S. M. Baker and S. M. Rowe, *JCI Insight*, 2019, **4**, 125954.

19 H. Frey and R. Haag, *Rev. Mol. Biotechnol.*, 2002, **90**, 257–267.

20 C. Nie, P. Pouyan, D. Lauster, J. Trimpert, Y. Kerkhoff, G. P. Szekeres, M. Wallert, S. Block, A. K. Sahoo, J. Dernedde, K. Pagel, B. B. Kaufer, R. R. Netz, M. Ballauff and R. Haag, *Angew. Chem., Int. Ed.*, 2021, **60**, 15870–15878.

21 P. Pouyan, C. Nie, S. Bhatia, S. Wedepohl, K. Achazi, N. Osterrieder and R. Haag, *Biomacromolecules*, 2021, **22**(4), 1545–1554.

22 I. Donskyi, M. Drüke, K. Silberreis, D. Lauster, K. Ludwig, C. Kühne, W. Unger, C. Böttcher, A. Herrmann, J. Dernedde, M. Adeli and R. Haag, *Small*, 2018, **14**, 1800189.

23 M. F. Gholami, D. Lauster, K. Ludwig, J. Storm, B. Ziem, N. Severin, C. Böttcher, J. P. Rabe, A. Herrmann, M. Adeli and R. Haag, *Adv. Funct. Mater.*, 2017, **27**, 1606477.

24 K. Silberreis, N. Niesler, N. Rades, R. Haag and J. Dernedde, *Biomacromolecules*, 2019, **20**, 3809–3818.

25 J. Dernedde, A. Rausch, M. Weinhart, S. Enders, R. Tauber, K. Licha, M. Schirner, U. Zügel, A. von Bonin and R. Haag, *Proc. Natl. Acad. Sci. U. S. A.*, 2010, **107**, 19679.

26 K. Achazi, R. Haag, M. Ballauff, J. Dernedde, J. N. Kizhakkedathu, D. Maysinger and G. Multhaup, *Angew. Chem., Int. Ed.*, 2021, **60**, 3882–3904.

27 M. Wallert, J. Plaschke, M. Dimde, V. Ahmadi, S. Block and R. Haag, *Macromol. Mater. Eng.*, 2021, **306**, 2000688.

28 B. Thongrom, A. Sharma, C. Nie, E. Quaas, M. Raue, S. Bhatia and R. Haag, *Macromol. Biosci.*, 2022, **22**, 2100507.

29 D. Gröger, F. Paulus, K. Licha, P. Welker, M. Weinhart, C. Holzhausen, L. Mundhenk, A. D. Gruber, U. Abram and R. Haag, *Bioconjugate Chem.*, 2013, **24**, 1507–1514.

30 K. Peng, Y. Gao, P. Angsantikul, A. LaBarbiera, M. Goetz, A. M. Curreri, D. Rodrigues, E. E. L. Tanner and S. Mitragotri, *Adv. Healthcare Mater.*, 2021, **10**, 2002192.

31 M. Gentzsch, S. E. Boyles, C. Cheluvaraju, I. G. Chaudhry, N. L. Quinney, C. Cho, H. Dang, X. Liu, R. Schlegel and S. H. Randell, *Am. J. Respir. Cell Mol. Biol.*, 2017, **56**, 568–574.

32 A. Balázs, P. Millar-Büchner, M. Mülleder, V. Farztdinov, L. Szyrwiel, A. Addante, A. Kuppe, T. Rubil, M. Drescher, K. Seidel, S. Stricker, R. Eils, I. Lehmann, B. Sawitzki, J. Röhmel, M. Ralser and M. A. Mall, *Front. Immunol.*, 2022, **13**, 822437.

33 M. Völler, A. Addante, H. Rulff, B. von Lospichl, S. Y. Gräber, J. Duerr, D. Lauster, R. Haag, M. Gradzielski and M. A. Mall, *Front. Physiol.*, 2022, **13**, 912049.

34 K. A. Ramsey, Z. L. Rushton and C. Ehre, *J. Visualized Exp.*, 2016, **112**, 54153.

35 J. Schindelin, I. Arganda-Carreras, E. Frise, V. Kaynig, M. Longair, T. Pietzsch, S. Preibisch, C. Rueden, S. Saalfeld, B. Schmid, J.-Y. Tinevez, D. J. White, V. Hartenstein, K. Eliceiri, P. Tomancak and A. Cardona, *Nat. Methods*, 2012, **9**, 676–682.

36 J. Schindelin, C. T. Rueden, M. C. Hiner and K. W. Eliceiri, *Mol. Reprod. Dev.*, 2015, **82**, 518–529.

37 S. Roller, H. Zhou and R. Haag, *Mol. Diversity*, 2005, **9**, 305–316.

38 S. Ferber, G. Tiram, A. Sousa-Herves, A. Eldar-Boock, A. Krivitsky, A. Scomparin, E. Yeini, P. Ofek, D. Ben-Shushan, L. I. Vossen, K. Licha, R. Grossman, Z. Ram, J. Henkin, E. Ruppin, N. Auslander, R. Haag, M. Calderón and R. Satchi-Fainaro, *eLife*, 2017, **6**, e25281.

39 M. Dimde, F. Neumann, F. Reisbeck, S. Ehrmann, J. L. Cuellar-Camacho, D. Steinhilber, N. Ma and R. Haag, *Biomater. Sci.*, 2017, **5**, 2328–2336.

40 L. Schaupp, A. Addante, M. Völler, K. Fentker, A. Kuppe, M. Bardua, J. Duerr, L. Piehler, J. Röhmel, S. Thee, M. Kirchner, M. Ziehm, D. Lauster, R. Haag, M. Gradzielski, M. Stahl, P. Mertins, S. Boutin, S. Y. Graeber and M. A. Mall, *Eur. Respir. J.*, 2023, **62**, 2202153.

41 H. Koeppe, D. Horn, J. Scholz, E. Quaas, S. Schötz, F. Reisbeck, K. Achazi, E. Mohammadifar, J. Dernedde and R. Haag, *Int. J. Pharm.*, 2023, **642**, 123158.

42 F. Paulus, R. Schulze, D. Steinhilber, M. Zieringer, I. Steinke, P. Welker, K. Licha, S. Wedepohl, J. Dernedde and R. Haag, *Macromol. Biosci.*, 2014, **14**, 643–654.

43 G. L. Ellman, *Arch. Biochem. Biophys.*, 1959, **82**, 70–77.

44 S. Tate, G. MacGregor, M. Davis, J. A. Innes and A. P. Greening, *Thorax*, 2002, **57**, 926–929.

45 A. M. Al-Salem, Q. Saquib, M. A. Siddiqui, J. Ahmad and A. A. Al-Khedhairy, *Toxics*, 2020, **8**, 109.

46 L. Tartier, Y. L. McCarey, J. E. Biaglow, I. E. Kochevar and K. D. Held, *Cell Death Differ.*, 2000, **7**, 1002–1010.

47 N. N. Sanders, S. C. De Smedt, E. Van Rompaey, P. Simoens, F. De Baets and J. Demeester, *Am. J. Respir. Crit. Care Med.*, 2000, **162**, 1905–1911.

48 M. Dawson, D. Wirtz and J. Hanes, *J. Biol. Chem.*, 2003, **278**, 50393–50401.

49 K. D. Held and J. E. Biaglow, *Radiat. Res.*, 1994, **139**, 15–23.

50 Y. Wang, M. Misto, J. Yang, N. Gehring, X. Yu and B. Moussian, *Toxicol. Rep.*, 2021, **8**, 124–130.